International Journal of Heat and Technology
Vol. 43, No. 1, February, 2025, pp. 11-18
Journal homepage: http://iieta.org/journals/ijht

How Charge Arrangement Affects Heat Transfer in Chamber Furnaces During Steel Heating

Jarosław Boryca[1], Tomasz Wyleciał[1*], Dariusz Urbaniak[2], Henryk Otwinowski[2]

[1] Faculty of Production Engineering and Materials Technology, Czestochowa University of Technology, Czestochowa 42-201, Poland
[2] Faculty of Mechanical Engineering, Czestochowa University of Technology, Czestochowa 42-201, Poland

Corresponding Author Email: tomasz.wylecial@pcz.pl

https://doi.org/10.18280/ijht.430102

Received: 17 December 2024
Revised: 2 February 2025
Accepted: 16 February 2025
Available online: 28 February 2025

Keywords:
heating, steel charge, chamber furnace, equalization of temperatures, heat transfer conditions

ABSTRACT

The article presents calculations performed using a developed computer program concerning the heating of a flat charge of finite dimensions. Boundary conditions of the first kind were taken into account in the calculations. The relationships relating to heat transfer by radiation were used. The following quantities were taken into account in the heat exchange model: emissivity of the charge, combustion chamber and gas, radiation constants of the systems participating in the heat exchange and configuration factors characterizing the analyzed systems. The assumptions used in the calculations result from the operation of real metallurgical facilities. The calculations were performed for the process of temperature equalization in the cross-section of a steel charge in a chamber furnace at a constant surface temperature of the charge. The calculations took into account the variability of the thermo-physical parameters of the charge with increasing temperature. The temperature changes in the charge axis, furnace temperature and unit heat flux during heating were determined. An analysis of the influence of temperature change on the heat exchange conditions depending on the arrangement of the charge in the furnace chamber was carried out. Reducing the value of the unit heat flux supplied during heating determines the increase in the efficiency of the charge heating process.

1. INTRODUCTION

There is an undetermined flow of heat when heating the charge. Heat flux density varies depending on position and time. The variability of temperature as a function of time is related to the change in the temperature gradient. If the process under consideration is in flat plates, then heat flow is considered in a three-dimensional rectangular coordinate system. In flat plates with unlimited length and width, heat flow is considered only in the direction perpendicular to the surface [1-4].

The temperature change during transient one-dimensional heat conduction is described by the differential Fourier equation [1-3, 5-18]:

$$\frac{\partial t}{\partial \tau} = \bar{a} \cdot \frac{\partial^2 t}{\partial x^2} \quad (1)$$

where:
t - temperature, °C,
τ - time, s,
$\bar{a}$ - thermal diffusivity, m^2/s,
x - coordinate along the x axis, m.

There are many functions that satisfy the Fourier equation. Among the most common are products of the exponential function of time and the trigonometric function of position. Special solutions of the Fourier equation can be functions multiplied by a constant value, products of these functions and polynomial functions. The choice of equation is determined by the fulfillment of initial and boundary conditions, the former of which are related to time and characterize the temperature distribution at the moment from which the process is examined (τ=0), and the latter are related to the surface and determine the nature of temperature changes on the surface of the heated body or the interaction of the surface of the body with the surrounding atmosphere [5, 19]. The heat transfer process in furnaces is well presented by Zhang et al. [20]. This book describes how heat transfer is related to energy exchange, also covering efficiency characteristics.

Boundary conditions are divided into three types, depending on whether they are known [1-5, 21, 22]:

1) temperature distribution on the surface of the heated element (these conditions include the cases of constant surface temperature and linearly varying surface temperature) – boundary conditions of the first kind;

2) the heat flux flowing to the surface – boundary conditions of the second kind;

3) the temperature distribution of the surrounding medium (in particular, there may be a constant temperature of the medium and a linearly varying temperature of the medium) – boundary conditions of the third kind.

The article presents an analysis of the process of heating a

flat charge for boundary conditions of the first kind. For these conditions, it was decided to find a simple calculation tool that would allow its use in engineering calculations. The use of the demonstrated computer program allows for simple calculations of the heating of a flat charge for any of its positions on the furnace hearth.

2. BASICS OF HEATING A FLAT CHARGE

Boundary conditions of the first kind usually apply in the final phases of heating [3, 5]. They are used after preheating with a linear increase in surface temperature. Their purpose is to equalize the temperature across the cross-section of the charge.

Heating a plate with a known defect surface temperature can be carried out with different initial conditions. The most commonly considered initial conditions are an equalized temperature at the cross section and a parabolic temperature distribution [2, 5].

The paper considers the parabolic distribution of temperature at the initial moment.

Heating processes in the charge usually produce a larger temperature difference than the technology allows.

Therefore, it becomes necessary to anneal in the final heating stage, with constant surface temperature. The temperature of the charge at any point and after any heating time is described by the equation [5]:

$$t^{"} = t_p + \left(t'_{axis} - t_p\right) \cdot \sum_{l=1}^{\infty} \frac{4 \cdot (-1)^{l+1}}{\delta_l^3} \cdot cos\left(\delta_l \cdot \frac{x}{s}\right) \cdot exp\left(-\delta_l^2 \cdot \frac{\bar{a} \cdot \tau}{s^2}\right) \quad (2)$$

where:

$t^{"}$ - final temperature, °C,

t_p - temperature of the surface of the charge, °C,

t'_{axis} - initial temperature of the charge axis, °C,

δ_l - the roots of the function cos, $\delta_l = \frac{2 \cdot l - 1}{2} \cdot \pi$,

s - calculated thickness of the charge layer, m.

Eq. (2) can be presented in criterion form:

$$\frac{t^{"} - t_p}{t'_{axis} - t_p} = \frac{t_p - t^{"}}{t_p - t'_{axis}} = \phi_1\left(Fo, \frac{x}{s}\right) \quad (3)$$

where:

ϕ_1 - relative temperature,

Fo - Fourier number value, $Fo = \frac{\bar{a} \cdot \tau}{s^2}$.

The above Eqs. (2) and (3) are used to determine the charge temperature at any point in the charge and at any time during the heating process.

The function values ϕ_1 are provided in Figure 1.

For the axes, Eq. (3) transforms to the form of [5]:

$$\frac{t_p - t^{"}_{axis}}{t_p - t'_{axis}} = \frac{\Delta t^{"}}{\Delta t'} = \delta = f(Fo) \quad (4)$$

where:

$t^{"}_{axis}$ - final temperature of the charge axis, °C,

$\Delta t'$ - initial temperature difference across the cross-section of the charge, K,

$\Delta t^{"}$ - final temperature difference across the charge, K,

δ - degree of temperature equalization.

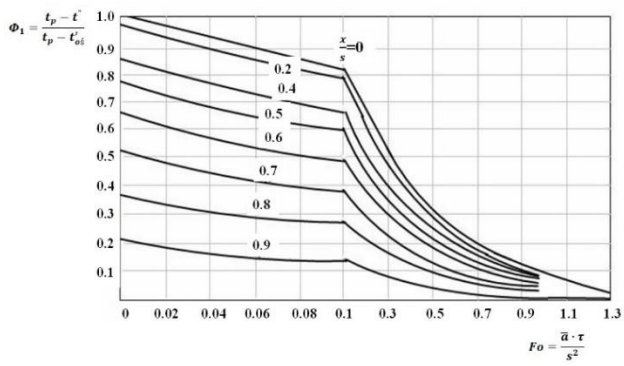

Figure 1. Relative temperatures ϕ_1 for the plate at constant surface temperature and parabolic initial temperature distribution [3, 5]

The value of the quotient of the final and initial temperature difference, denoted as δ, is called the degree of temperature equalization. It depends only on the value of the Fourier number. This relationship is shown graphically in Figure 2.

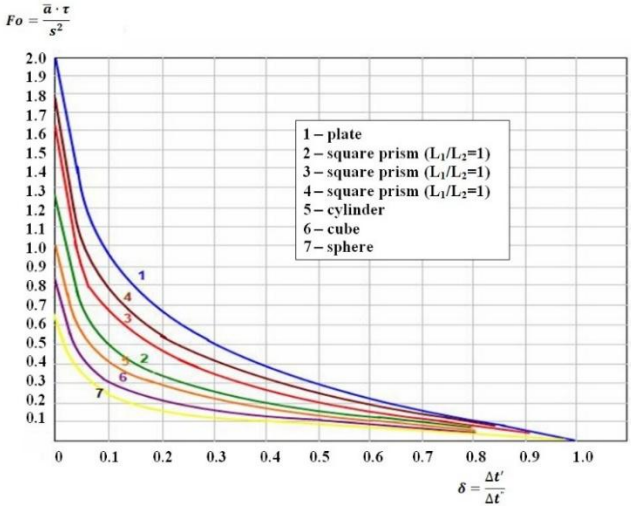

Figure 2. Dependence of the degree of temperature equalization on the Fourier number and shape of the charge [3, 5]

Determining δ value allows determining the heating time for specific temperature differences at the beginning and end of heating by determining *Fo* number value. The graph shown in Figure 2 can also be used to determine the temperature in the charge axis at any time during heating.

If Fo≥0.06 then the temperature at the axis for an unlimited plate can be calculated from the following relationship [5]:

$$\frac{t_p - t^{"}_{axis}}{t_p - t'_{axis}} = 1.03 \cdot exp\left(-2.47 \cdot \frac{\bar{a} \cdot \tau}{s^2}\right) \quad (5)$$

The unit heat flux is determined by the relationship [5, 13]:

$$\frac{\dot{q} \cdot s}{\lambda \cdot \Delta t'} = F(Fo) \quad (6)$$

where:

$\dot{q}$ - unit heat flux, W/m^2,

λ - thermal conductivity coefficient, W/(m·K),

$\Delta t'$ - initial temperature difference across the cross-section of the charge, K,

F(Fo) - the value of the function depends on the Fourier number.

The value of the *F*(*Fo*) function is provided in Figure 3.

Determining the value of the function *F*(*Fo*) depending on the *Fo* number (Figure 3) allows calculating the heat flux density at any time during the heating process using Eq. (4).

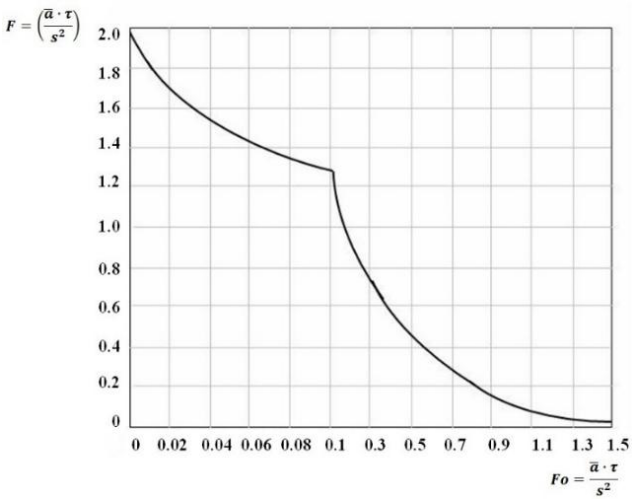

Figure 3. Function *F*(*Fo*) for calculating heat flux density at constant plate surface temperature [3, 5]

The furnace temperature can be calculated from the equation [5, 12]:

$$t_{furnace} = 100 \cdot \sqrt[4]{\frac{\dot{q}}{C_{p-m}} + \left(\frac{T_p}{100}\right)^4} - 273 \tag{7}$$

where:

C_{p-m} - radiation constant of the furnace-metal system, W/(m^2 K^4),

T_p - surface temperature of the charge, K.

The radiation constant of the furnace-metal system is determined by the relationship [3, 12]:

$$C_{p-m} = C_0 \cdot \varepsilon_{p-m} \cdot \varphi_{m-ś} \tag{8}$$

where:

C_0 - the black body radiation constant, $C_0 = 5{,}67$ W/(m^2·K^4),

ε_{p-m} - equivalent emissivity of the furnace-metal system,

$\varphi_{m-ś}$ - angular radiation coefficient of the metal-furnace surface system.

The emissivity of the furnace-metal system is determined from the relationship [3, 12]:

$$\varepsilon_{p-m} = \frac{\varepsilon_m}{1 - \varphi_{m-m} \cdot (1 - \varepsilon_m)} \tag{9}$$

where:

ε_m - equivalent emissivity of the metal,

φ_{m-m} - angular radiation coefficient of the metal-metal system.

The relationship (9) shows that the emissivity of the furnace-metal system depends on the configuration factor and the emissivity of the charge, which is a property characteristic of the heated material and does not depend on the furnace atmosphere. The configuration coefficients of the metal-metal system and the metal-furnace surface system are a function of geometric parameters: Dimensions and arrangement of the charge and dimensions of the furnace working chamber.

The configuration factors are determined from the following relationships [3, 12, 17, 23-25]:

$$\varphi_{m-m} = \varphi_{ś-m} = \frac{A_m}{A} \tag{10}$$

where:

A_m - the surface of the metal (steel charge) participating in heat transfer, m^2,

A - total heat transfer surface (metal and furnace surface), m^2.

$$\varphi_{m-ś} = \varphi_{ś-ś} = 1 - \varphi_{m-m} \tag{11}$$

Using Eqs. (8), (9), (10) and (11) and substituting the calculated values into Eq. (7) allows the furnace temperature to be determined at any time during the charge heating process.

More extensive theoretical considerations for the process of heating the charge at a constant surface temperature are included in the works [2, 3, 5].

3. CALCULATION ASSUMPTIONS

It was assumed that a finite-size charge of medium-carbon steel was heated in the chamber furnace. The charge is heated unilaterally toward the furnace hearth at a constant surface temperature. In other directions, the heating is bilateral.

The following technological assumptions were made for the calculations:

- charge surface temperature t_p=1180°C,
- initial temperature in the axis of the charge t'_{axis}=840°C,
- final temperature in the axis of the charge t''_{axis}=1150°C.

Other calculation assumptions:

- dimensions of the flat charge *a*=0.6 m, *b*=0.8 m, *l*=1.2 m,
- furnace dimensions *L* =1.8 m, *B*= 1.4 m, *H*=1.6 m,
- batch density ρ=7850 kg/m^3,
- number of charges in the oven *n*=1,
- emissivity of the charge ε_m=0.8.

The basis for the adopted calculation assumptions was the authors' own extensive experience with real objects. In addition, the adopted assumptions made it possible to take into account the influence of the charge arrangement on the heat exchange process inside the furnace. The limitations of the adopted assumptions may be the geometry of the charge and furnace and the insulation of the hearth.

The values of material parameters (λ, $\bar{a}$) of the charge were calculated for the average temperature:

$$t_{śr} = \frac{2 \cdot t_p + t'_{axis} + t''_{axis}}{4} \tag{12}$$

where:

$t_{śr}$ - average temperature, °C.

The method of laying the charge on the insulated furnace hearth, for the variants considered, is shown in Figures 4-6.

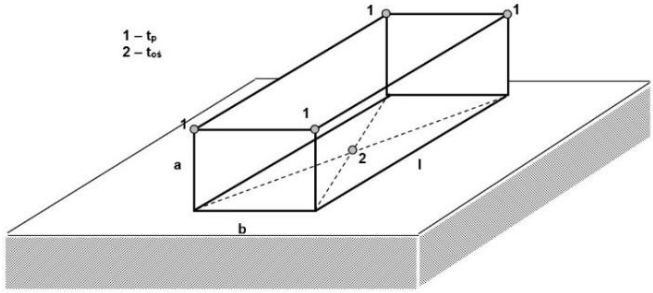

Figure 4. Method of placing the charge on the insulated hearth for variant I (t_p – temperature of the charge surface, °C, t_{axis} - temperature in the axis of the charge – surface adjacent to the insulated hearth, °C)

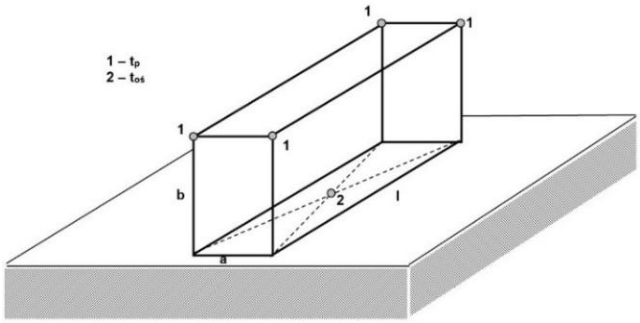

Figure 5. Method of placing the charge on the insulated hearth for variant II (t_p - temperature of the charge surface, °C, t_{axis} - temperature in the axis of the charge - surface adjacent to the insulated hearth, °C)

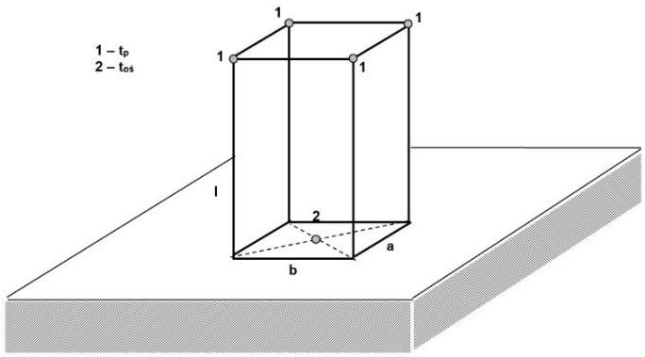

Figure 6. Method of placing the charge on the insulated hearth for variant III (t_p - temperature of the charge surface, °C, t_{axis} - temperature in the axis of the charge - surface adjacent to the insulated hearth, °C)

4. CALCULATION METHODOLOGY

Theoretical relationships for heating the charge were used for developing a computer program for computations. To perform the heating calculations, it was required to develop mathematical functions describing the variability of the thermo-physical properties of the charge with the average temperature of the charge over a given reheating period.

These properties include:

- thermal conductivity coefficient λ, W/(m·K),
- temperature equalization coefficient a, m^2/h.

Based on the data in the paper, mathematical functions were established for the medium-carbon steel charge.

In the analyzed case, for the respective ranges of average temperature, the following relationships were used [26]:

- for 0°C≤t_{sr}<800°C

$$\lambda = 50.79821 - 0.00992 \cdot t_{śr} - 2.518 \cdot 10^{-5} \cdot t_{śr}^2 \quad (13)$$

- for 800°C≤t_{sr}<900°C

$$\lambda = 26.1 - 0.001 \cdot (900 - t_{śr}) \quad (14)$$

- for 900°C≤t_{sr}<1200°C

$$\lambda = 34.465 - 0.02505 \cdot t_{śr} - 1.75 \cdot 10^{-5} \cdot t_{śr}^2 \quad (15)$$

- for t_{sr}≥1200°C

$$\lambda = 29.6 \quad (16)$$

where:

λ – thermal conductivity, W/(m·K).

The thermal diffusivity a can be described, for the respective ranges of average temperature, with the following relationships [22]:

- for 0°C≤t_{sr}<700°C

$$\bar{a} = 0.052 - 4.82143 \cdot 10^{-5} \cdot t_{sr} \quad (17)$$

- for 700°C≤t_{sr}<800°C

$$\bar{a} = 0.018 \quad (18)$$

- for 800°C≤t_{sr}<900°C

$$\bar{a} = 0.018 - 2 \cdot 10^{-5} \cdot (t_{sr} - 800) \quad (19)$$

- for t_{sr}≥900°C

$$\bar{a} = 0.02 \quad (20)$$

To determine the total heating time for a flat charge, the relationship was transformed for a prism with dimensions 2s×2b×2l [3, 5]:

$$\frac{t_p - t''_{axis}}{t_p - t'} = 2.05 \cdot exp\left[-2.47 \cdot \left(\frac{\bar{a} \cdot \tau}{s^2} + \frac{\bar{a} \cdot \tau}{b^2} + \frac{\bar{a} \cdot \tau}{l^2}\right)\right] \quad (21)$$

to a form corresponding to the assumptions used in the calculations:

- for variant I:

$$\tau = \frac{ln\left(\frac{\delta}{2.05}\right)}{\left[-2.47 \cdot \left(\frac{\bar{a}}{a^2} + \frac{\bar{a}}{\left(\frac{b}{2}\right)^2} + \frac{\bar{a}}{\left(\frac{l}{2}\right)^2}\right)\right]} \quad (22)$$

- for variant II:

$$\tau = \frac{ln\left(\frac{\delta}{2.05}\right)}{\left[-2.47 \cdot \left(\frac{\bar{a}}{b^2} + \frac{\bar{a}}{\left(\frac{a}{2}\right)^2} + \frac{\bar{a}}{\left(\frac{l}{2}\right)^2}\right)\right]} \quad (23)$$

- for variant III:

$$\tau = \frac{ln\left(\frac{\delta}{2.05}\right)}{\left[-2.47 \cdot \left(\frac{\bar{a}}{l^2} + \frac{\bar{a}}{\left(\frac{b}{2}\right)^2} + \frac{\bar{a}}{\left(\frac{a}{2}\right)^2}\right)\right]} \quad (24)$$

For all variants, the function δ denoted the ratio of temperature differences consistent with Eq. (4).

Based on the described functions and relationships, a computer calculation program was developed. A view of the program window is shown in Figure 7.

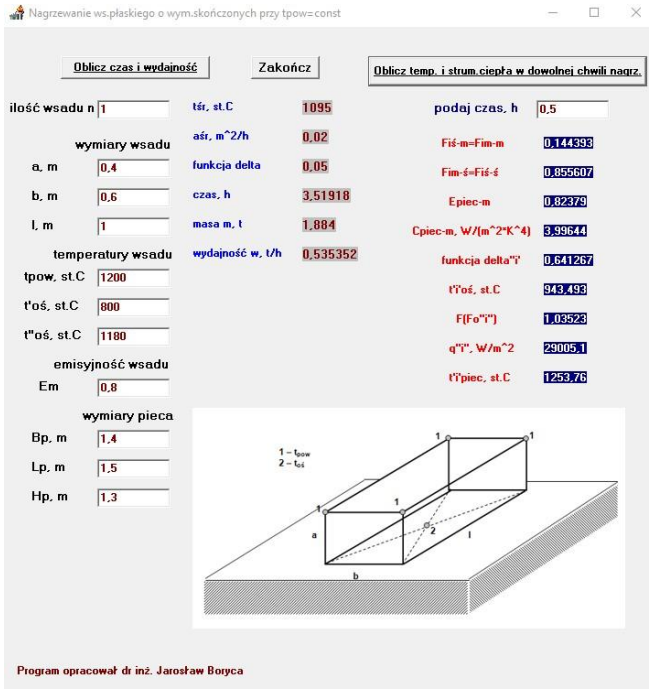

Figure 7. View of the program window

5. CALCULATION RESULTS AND THEIR ANALYSIS

For the assumed variants, calculations of the heating process were carried out using the developed computer program. The results of the supporting calculations are shown in Tables 1-3.

Table 1. Results of supporting calculations of the heating process for variant I

Size	Value
Average temperature t_{sr}, °C	1087.5
Temperature compensation factor $\bar{a}$, m²/h	0.02
Capacity w, t/h	0.838
Configuration factor of the wall-to-metal and metal-to-metal system $\varphi_{ś-m} = \varphi_{m-m}$	0.190
Configuration factor of the metal-wall and wall-to-wall system $\varphi_{m-ś} = \varphi_{ś-ś}$	0.810
Emissivity of the furnace-metal system ε_{p-m}	0.832
Radiation constant of the furnace-metal system C_{p-m}, W/(m²·K⁴)	3.82

Table 2. Results of supporting calculations of the heating process for variant II

Size	Value
Average temperature t_{sr}, °C	1087.5
Temperature equalization coefficient $\bar{a}$, m²/h	0.02
Capacity w, t/h	1.097
Configuration factor of wall-to-metal and metal-to-metal system $\varphi_{ś-m} = \varphi_{m-m}$	0.198
Configuration factor of the metal-wall and wall-to-wall system $\varphi_{m-ś} = \varphi_{ś-ś}$	0.802
Emissivity of the furnace-metal system ε_{p-m}	0.833
Radiation constant of the furnace-metal system C_{p-m}, W/(m²·K⁴)	3.79

Table 3. Results of supporting calculations of the heating process for variant III

Size	Value
Average temperature t_{sr}, °C	1087.5
Temperature compensation factor $\bar{a}$, m²/h	0.02
Capacity w, t/h	1.28
Configuration factor of wall-to-metal and metal-to-metal system $\varphi_{ś-m} = \varphi_{m-m}$	0.206
Configuration factor of the metal-wall and wall-to-wall system $\varphi_{m-ś} = \varphi_{ś-ś}$	0.794
Emissivity of the furnace-metal system ε_{p-m}	0.834
Radiation constant of the furnace-metal system C_{p-m}, W/(m²·K⁴)	3.76

The detailed results of the calculations, including time intervals for each alternative, are summarized in Tables 4-6.

Table 4. The detailed results of the calculations, including time intervals for variant I

τ, h	δ	t_{axis}, °C	$F(Fo)$	$\dot{q}$, W/m²	$t_{furnace}$, °C
0	1.0516	840	1.6276	25750	1232
0.5	0.8001	908	1.3311	21059	1223
1.0	0.6087	973	1.0886	17223	1215
1.5	0.4631	1023	0.8903	14086	1209
2.0	0.3524	1060	0.7281	11520	1204
2.5	0.2681	1089	0.5955	9421	1200
3.0	0.2040	1111	0.4870	7705	1196
3.5	0.1552	1127	0.3983	6301	1193
4.0	0.1181	1140	0.3257	5154	1191
4.5	0.0898	1150	0.2664	4215	1189

Table 5. The detailed results of the calculations, including time intervals for variant II

τ, h	δ	t_{axis}, °C	$F(Fo)$	$\dot{q}$, W/m²	$t_{furnace}$, °C
0	1.0516	840	1.6276	19312	1220
0.5	0.7353	930	1.4535	17247	1216
1.0	0.5142	1005	1.2980	15402	1212
1.5	0.3595	1057	1.1592	13755	1209
2.0	0.2514	1094	1.0352	12284	1206
2.5	0.1758	1120	0.9245	10970	1203
3.0	0.1229	1138	0.8256	9797	1201
3.5	0.0859	1151	0.7373	8749	1199

Changes in the degree of temperature equalization over time for each variant are shown in Figure 8, while changes in function $F(Fo)$ - in Figure 9.

Table 6. The detailed results of the calculations, including time intervals for variant III

τ, h	δ	t_{axis}, ℃	$F(Fo)$	$\dot{q}$, W/m²	$t_{furnace}$, ℃
0	1.0516	840	1.6276	12874	1207
0.5	0.6923	945	1.5478	12243	1206
1.0	0.4557	1025	1.4719	11643	1205
1.5	0.3000	1078	1.3997	11072	1204
2.0	0.1975	1113	1.3311	10530	1202
2.5	0.1300	1136	1.2658	10013	1201
3.0	0.0856	1151	1.2038	9522	1200

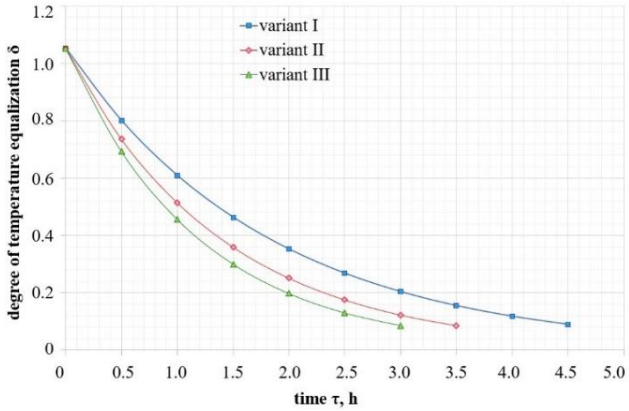

Figure 8. Distribution of the degree of temperature equalization during heating for the respective variants

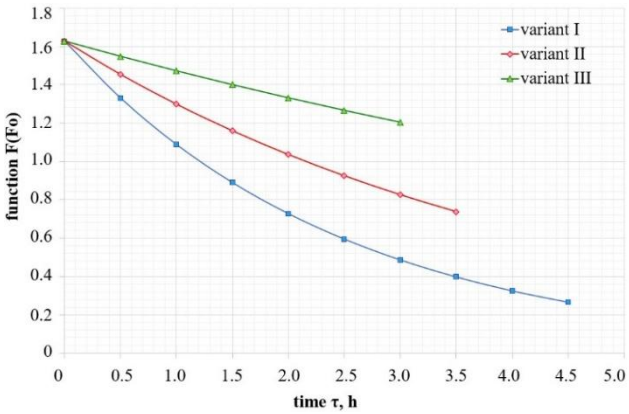

Figure 9. Distribution of functions $F(Fo)$ during heating time for each variant

The temperature distribution during heating for each variant is shown in Figures 10-12.

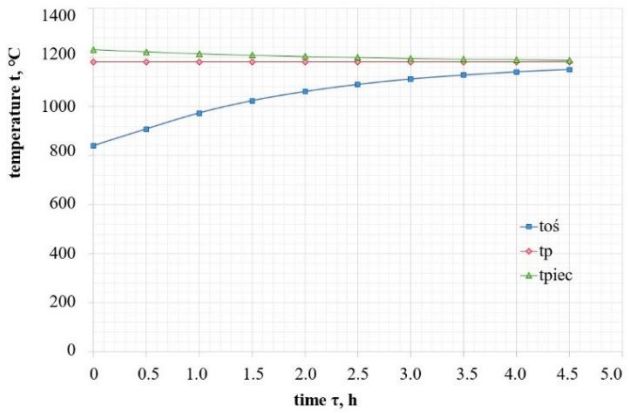

Figure 10. Temperature distribution during heating for variant I

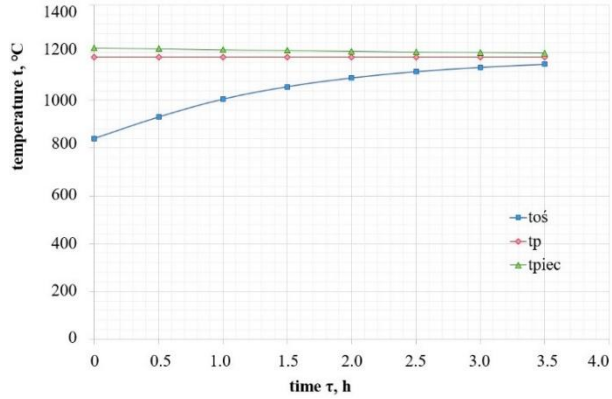

Figure 11. Temperature distribution during heating for variant II

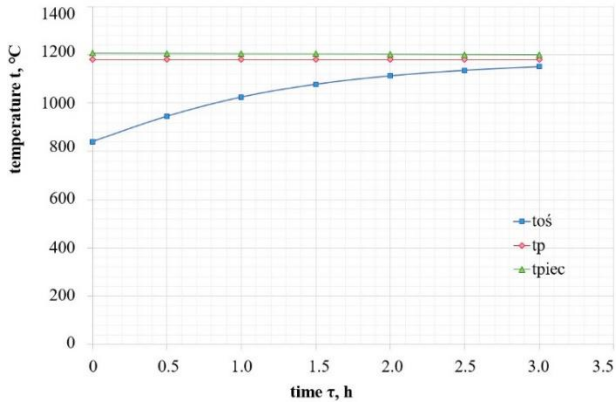

Figure 12. Temperature distribution during heating for variant III

The distribution of unit heat flux over time for each variant is shown in Figure 13.

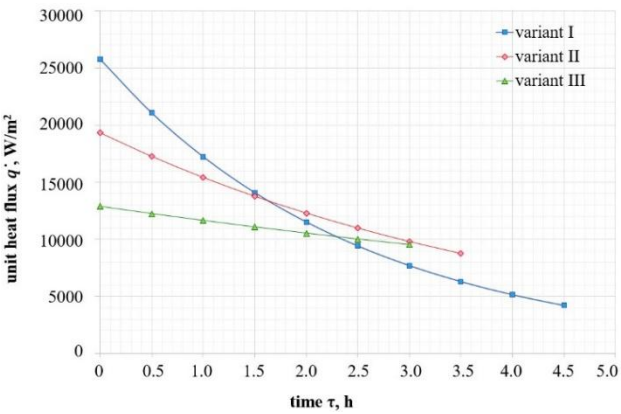

Figure 13. Distribution of unit heat flux during heating for each variant

Three types of stacking the charge on an insulated furnace hearth were analyzed. For variant I, the contact area with the hearth is the largest at 0.96 m² (l×b). This case, on the other hand, is characterized by the smallest contact area with the gas solid of 3.36 m². For variant II, the contact area with the hearth is 0.72 m² (l×a). In turn, this case is characterized by the contact area with the gas solid of 3.60 m². For variant III, the contact area with the hearth is the smallest at 0.48 m² (a×b). In turn, this case is characterized by the largest contact area with the gas solid of 3.84 m². Therefore, it can be concluded that the

arrangement of the charge in the furnace chamber determines the heat transfer surface area.

Analyzing the calculation results for the different variants, it is also noted that the configuration factor of the wall-to-metal and metal-to-metal system $\varphi_{ś-m} = \varphi_{m-m}$ increases with the increase of the heat transfer surface area of the charge. However, the configuration factor of the metal-wall and wall-to-wall system decreases $\varphi_{m-ś} = \varphi_{ś-ś}$.

As the heat transfer surface area of the charge increases, the emissivity of the furnace-metal system increases ε_{p-m} and the radiation constant of the furnace-metal system decreases C_{p-m}.

The thickness of the exhaust layer for each variant was analyzed using the relationship:

$$\delta_{sp} = \frac{3.6 \cdot V}{A_w} = \frac{3.6 \cdot (B \cdot L \cdot H - a \cdot b \cdot l)}{2 \cdot (B \cdot L + B \cdot H + L \cdot H) + A_b} \qquad (25)$$

where:
δ_{sp} - thickness of the exhaust layer, m,
V - volume of the gas solid (flue gas), m^3,
A_w - total contact area of the charge and heating chamber with the gas solid (flue gas), m^2,
A_b -lateral area of the charge, m^2.
The results of the calculations are as follows:

- for variant I $\delta_{sp} = 0.704\ m$,
- for variant II $\delta_{sp} = 0.685\ m$,
- for variant III $\delta_{sp} = 0.668\ m$.

This leads to the conclusion that the arrangement of the charge determines the thickness of the flue gas layer. By increase the heat transfer surface of the charge, the thickness of the flue gas layer decreases, and this affects the emissivity of the flue gas.

Another extremely important aspect is the efficiency of the heating process, which increases with an increase in the heat transfer surface area of the charge, and is highest for variant III. This is directly related to the fact that the heating time decreases with an increase in the heat transfer surface area of the charge.

When considering the charge heating functions for boundary conditions of the first kind, it can be seen that the temperature stabilization coefficient δ reaches lower values for variants with a larger charge heat transfer area, while the function $F(Fo)$ reaches higher values for variants with a larger charge heat transfer area.

Analyzing the distribution of unit heat flux over time, it can be concluded that for variant III, the curve is most flattened, i.e. it has the smallest difference in value between the beginning and end of heating. In the case of variant I, the situation is reversed, i.e. the difference in unit heat flux between the beginning and end of heating is the greatest.

Taking into account the extreme values, the average values of the unit heat flux for the respective variants are:

- for variant I $\dot{q}_{śr} = 14983\ \frac{W}{m^2}$,
- for variant II $\dot{q}_{śr} = 14031\ \frac{W}{m^2}$,
- for variant III $\dot{q}_{śr} = 11198\ \frac{W}{m^2}$.

Therefore, it can be concluded that an increase in efficiency is equivalent to a decrease in the value of the unit heat flux.
Different efficiencies were obtained for the variants presented. The lowest efficiency was obtained for variant I with the smallest charge heat transfer area (w=0.838 t/h), while the highest value was obtained for variant III with the largest charge heat transfer area (w=1.280 t/h).

The value of the heat transfer surface area of the charge (the arrangement of the charge in the furnace) determines the charge heating functions, configuration factors, the emissivity of the furnace-metal system and the emissivity of the gas, and the radiation constant of the furnace-metal system. For the highest-efficiency variant, there is a rapid increase in both the temperature in the axis of the charge with a more rapid decrease in furnace temperature than for lower efficiencies.

For variant I, the increase in the temperature of the medium is more spread out over time. Comparing the performance for technologies I, II and III, it can be seen that the variant for which the furnace temperature gradient (start and end of heating) is the smallest, has the highest efficiency. The course of the heating curves is determined by the value of the unit heat flux. In each case, the flux decreases over time, but the largest jump is seen for variant I, while the smallest one - for variant III.

6. CONCLUSIONS

Based on the theoretical analysis and the calculations performed, the following conclusions can be drawn:

- For a given heating technology (a given variant of charge stacking), heat consumption is determined by the value of the heat transfer surface of the charge.
- The heat transfer surface area of the charge has a decisive effect on performance in the process of heating with a constant charge surface temperature, that is according to boundary conditions of the first kind.
- The value of the heat transfer surface area of the charge (the arrangement of the charge in the furnace) determines the charge heating functions, configuration factors, the emissivity of the furnace-metal system and the emissivity of the gas, and the radiation constant of the furnace-metal system.
- An increase in the efficiency of the charge heating process results in a decrease in specific heat consumption.

REFERENCES

[1] Kieloch, M., Słupek, S., Wyczółkowski, S., Wyczółkowski, R. (2002). Energy-saving and small-scale heating of steel charge. Scientific Papers of the Department of Process Engineering, Materials Science and Applied Physics, Series Metallurgy No. 29.

[2] Kieloch M. (2010). Rationalization of charge heating. Scientific Papers of the Department of Process Engineering, Materials Science and Applied Physics, Series Monographs No. 8.

[3] Senkara, T. (1981). Calculations of thermal heating furnaces in metallurgy. Śląsk, Katowice.

[4] Szecówka, L. (2006) Heat exchange by radiation in the working space of industrial furnaces. Częstochowa University of Technology Publishing House.

[5] Kieloch, M. (1995). Echnology and principles of charge heating calculations. Częstochowa University of Technology Publishing House, Częstochowa.

[6] Hahn, D.W., Necati Özişik, M. (2012). Heat Conduction. John Wiley & Sons, Inc., Hobolen, New Jersey.

[7] Han, J.C., Wright, L.M. (2022). Analytical Heat Transfer. Taylor & Francis. https://library.oapen.org/handle/20.500.12657/79393.

[8] Mihir, S. (2017). Analytical heat transfer. University of Notre Dame, Notre Dame.
[9] Kostowski, E. (2000). Heat flow. Silesian Polish Publishing House, Gliwice.
[10] Kieloch, M., Kruszyński, S., Boryca, J., Piechowicz, Ł. (2006). Thermodynamics and thermal engineering, calculation exercises. Częstochowa University of Technology Script, Częstochowa.
[11] Słupek, S., Nocoń, J., Buczek, A. (2002). Thermal Technology - Computational Exercises. AGH Publishing House, Cracow.
[12] Boryca J. (2024). Computer calculation program for heating the cylinder at a constant surface temperature of the charge. Advances in Thermal Processes and Energy Transformation, 7(1): 1-4. https://doi.org/10.54570/atpet2024/07/01/0001
[13] Marín, E. (2011). Does Fourier's law of heat conduction contradict the theory of relativity? Latin-American Journal of Physics Education, 5(2): 402-405. http://www.lajpe.org/june11/13_LAJPE_519_Ernesto_ Marin_Preprint_corr_f.pdf.
[14] Song C.H. (2013). Thermal Engineering, Machinery Industry Press, Beijing.
[15] Wang, Y., Wang, P. (2022). Application of Fourier's law in one-dimensional steady heat conduction calculation of cylinder wall. Journal of Physics: Conference Series, 2381: 012002. https://doi.org/10.1088/1742-6596/2381/1/012002
[16] Logan J.D. (2015). Applied Partial Differential Equations. Springer Verlag, New York.
[17] Qu, Z., Wang, D., Ma, Y. (2017). Nondiffusive thermal transport and prediction of the breakdown of Fourier's law in nanograting experiments. AIP Advances, 7(1): 015108. https://doi.org/10.1063/1.4973331
[18] Wiśniewski, S., Wiśniewski, T.S. (2020). Heat Exchange. WNT, Warszawa.
[19] Kieloch, M., Krężołek, I. (1988). Heat Transfer and Mass Transfer in Environmental Engineering. WNT: Warsaw, Poland.
[20] Zhang, Y., Li, Q., Zhou, H. (2016). Theory and Calculation of Heat Transfer in Furnaces. Academic Press, Elsevier, Amsterdam. https://doi.org/10.1016/C2013-0-13233-3
[21] Shahnazari, M., Ahmadi, Z., Masooleh, L.S. (2017). Perturbation analysis of heat transfer and a novel method for changing the third kind boundary condition into the first kind. Journal of Porous Media, 20(5): 449-460. https://doi.org/10.1615/JPorMedia.v20.i5.60
[22] Tu, T.W. (2015). Exact solution of heat transfer in a plate with time-dependent boundary conditions of first kind. Data Journal of Aeronautics, Astronautics and Aviation, 47(2): 123-130. https://doi.org/10.1155/2015/203404
[23] Gołdasz, A., Malinowski, Z. (2016). Heat flux identification at the charge surface during heating in chamber furnace. Archives of Metallurgy and Materials, 61(4): 2021-2026. https://doi.org/10.1515/amm-2016-0326
[24] Hadała, B., Rywotycki, M., Malinowski, Z., Kajpust, S., Misiowiec, S. (2021). Optimization of long charge heating in a rotary furnace. Archives of Metallurgy and Materials, 66(2): 659-668, https://doi.org/10.24425/amm.2021.135904
[25] Yunus, A.Ç. (2007). Heat and Mass Transfer. McGrawHill, New York.
[26] Boryca, J., Kolmasiak, C., Wyczółkowski, R., Bagdasaryan, V., Aghbalyan, S. (2024). Calculation model of heating curves of a steel charge heated in a walking beam furnace before plastic working. Metalurgija, 63(3-4): 457-460.